Published in final edited form as:
J Geophys Res Atmos. 2018 ; 123(19): 11225–11237. doi:10.1029/2018JD029284.

Airborne Observations of Reactive Inorganic Chlorine and Bromine Species in the Exhaust of Coal-Fired Power Plants

Ben H. Lee[1], **Felipe D. Lopez-Hilfiker**[1,2], **Jason C. Schroder**[3,4], **Pedro Campuzano-Jost**[3,4], **Jose L. Jimenez**[3,4], **Erin E. McDuffie**[3,4,5], **Dorothy L. Fibiger**[5], **Patrick R. Veres**[5], **Steven S. Brown**[4,5], **Teresa L. Campos**[6], **Andrew J. Weinheimer**[6], **Frank F. Flocke**[6], **Gary Norris**[7], **Kate O'Mara**[7], **Jaime R. Green**[8,9], **Marc N. Fiddler**[9], **Solomon Bililign**[8,9], **Viral Shah**[1], **Lyatt Jaeglé**[1], and **Joel A. Thornton**[1]

[1]Department of Atmospheric Sciences, University of Washington, Seattle, WA, USA [2]Now at Paul Scherrer Institute, Villigen, Switzerland [3]Cooperative Institute for Research in Environmental Sciences, University of Colorado Boulder, Boulder, CO, USA [4]Department of Chemistry, University of Colorado Boulder, Boulder, CO, USA [5]Earth System Research Laboratory, Chemical Sciences Division, National Oceanic and Atmospheric Administration, Boulder, CO, USA [6]National Center for Atmospheric Research, Boulder, CO, USA [7]U.S. Environmental Protection Agency, Research Triangle, NC, USA [8]Department of Physics, North Carolina Agricultural and Technical State University, Greensboro, NC, USA [9]NOAA-ISET Center, North Carolina Agricultural and Technical State University, Greensboro, NC, USA

Abstract

We present airborne observations of gaseous reactive halogen species (HCl, Cl_2, $ClNO_2$, Br_2,$BrNO_2$, and BrCl), sulfur dioxide (SO_2), and nonrefractory fine particulate chloride (pCl) and sulfate(pSO_4) in power plant exhaust. Measurements were conducted during the Wintertime INvestigation of Transport, Emissions, and Reactivity campaign in February–March of 2015 aboard the NCAR-NSF C-130 aircraft. Fifty air mass encounters were identified in which SO_2 levels were elevated ~5 ppb above ambient background levels and in proximity to operational power plants. Each encounter was attributed to one or more potential emission sources using a simple wind trajectory analysis. In case studies, we compare measured emission ratios to those reported in the 2011 National Emissions Inventory and present evidence of the conversion of HCl emitted from power plants to $ClNO_2$. Taking into account possible chemical conversion downwind, there was general agreement between the observed and reported HCl: SO_2 emission ratios. Reactive bromine species (Br_2, $BrNO_2$, and/or BrCl) were detected in the exhaust of some coal-fired power plants, likely related to the absence of wet flue gas desulfurization emission control technology. Levels of bromine species enhanced in some encounters exceeded those expected assuming all of the native bromide in coal was released to the atmosphere, though there was no reported use of bromide salts (as a way to reduce mercury emissions) during Wintertime INvestigation of Transport, Emissions, and Reactivity observations. These measurements represent the first ever in-flight observations of reactive gaseous chlorine and bromine containing compounds present in coal-fired power plant exhaust.

1. Introduction

Reactive halogen species, as oxidizing agents in the troposphere, affect the lifetimes of volatile organic compounds, nitrogen oxides (NO_x), ozone (O_3), and mercury (Hg) (Saiz-Lopez & von Glasow, 2012) and represent components of the O_3 budget (Read et al., 2008; Schroeder et al., 1998). Uncertainties in their sources and multiphase recycling limit accurate assessment of their regional and global impacts on the processes listed above (Rossi, 2003; Simpson et al., 2015). The detection of elevated levels of nitryl chloride ($ClNO_2$) in moderately polluted nighttime atmospheres in both marine- and continental-influenced regions (Mielke et al., 2011; Osthoff et al., 2008; Riedel et al., 2012, 2013; Thornton et al., 2010; Young et al., 2012), for instance, has renewed efforts to determine sources of reactive chlorine, which occur mostly in the form of HCl and particulate chloride (pCl). Given the solubility of HCl and its dependence upon particle acidity, HCl and aqueous pCl exist in a thermodynamic equilibrium. Sources of either one, therefore, can influence multiphase chlorine activation chemistry, which leads to $ClNO_2$ or Cl_2 production (Behnke et al., 1997; Finlayson-Pitts et al., 1989; Roberts et al., 2008; Vogt et al., 1996).

The only available global inventory suggests that approximately 80% of the 62 Tg of gaseous HCl produced per year originates from the ocean (Keene et al., 1999), whereby HCl is displaced from chloride-containing sea salt aerosol to the gas phase with increasing particle acidification (Clegg & Brimblecombe, 1985; Crisp et al., 2014; Robbins et al., 1959). The rest of the global burden is thought to largely originate from combustion processes, including cement production, waste incineration, biomass burning, and coal combustion for electricity generation (McCulloch et al., 1999), as trace amounts of organic and inorganic chloride present within the fuel are converted mostly to HCl during combustion. Anthropogenic HCl emissions are thought to be on a downward trend in the United States over the past few decades, reflecting those of SO_2 and consistent with the decline in the use of coal for electricity generation and the implementation of desulfurization technology (United States Office of Energy Markets and End Use), but top-down validation of the emission ratios by direct atmospheric measurements is lacking. On the other hand, the practice of adding halides to coal fuel—mainly as calcium bromide or iodide in solution to curb mercury emissions (Reisch, 2015)—have increased the likelihood of halides being released to the environment. Though elevated bromide levels have been documented in the water environment impacted by the wastewater discharged from coal-fired power plants (Good & VanBriesen, 2016; McTigue et al., 2014; U.S. EPA, 2015), their abundance and composition in the gas exhaust have yet to be determined. Modeling studies on HOCl emissions from power plants have shown significant potential impact on regional photochemistry (Chang et al., 2002; Chang & Allen, 2006; Tanaka et al., 2003); however, speciated measurements of the suite of halogen compounds that are potentially emitted by coal-fired power plants are lacking.

The Wintertime INvestigation of Transport, Emissions, and Reactivity (WINTER) experiment, which utilized the highly instrumented NCAR/NSF C-130 aircraft based out of Norfolk, VA, provided the opportunity to study emissions from power generation plants during the winter season when chemistry and boundary layer dynamics behave differently than during the more often studied summer season. We describe a simple wind trajectory-

based approach to attribute each polluted air mass encounter—characterized by sharp enhancements in time of SO_2 nearby operational power plants—to one or more potential emission sources. The information documented in the National Emissions Inventory (NEI) 2011 provided a priori estimates of HCl:SO_2 emission ratios to compare against those observed during WINTER for the polluted air mass encounters which were able to be attributed to a single operating power plant (https://www.epa.gov/air-emissions-inventories/national-emissions-inventory-nei). We assess the factors that may have influenced why hydrogen chloride (presumably the most abundant of the chlorine-containing gaseous species emitted from coal combustion) and reactive bromine (Br_2, BrCl, and $BrNO_2$) species were measured (or not measured despite elevated SO_2 levels) in power plant exhaust.

2. Methods

Mixing ratios of HCl, HOCl, Cl_2, $ClNO_2$, Br_2, $BrNO_2$, BrCl, and SO_2 were measured during WINTER using the University of Washington iodide-adduct high-resolution time of flight chemical ionization spectrometer (HRToF-CIMS) aboard the NSF/NCAR C-130 aircraft. The University of Washington HRToF-CIMS instrument is identical in concept to that described by Lee et al. (2014) that flew previously aboard the NOAA P-3 aircraft during the Southeast Nexus campaign (Warneke et al., 2016) but with modifications implemented for the WINTER 2015 experiment. Details of these modifications are provided by Lee et al. (2018). In summary, ambient air is continuously drawn into the HRToF-CIMS through a 40-cm long 1.6-cm inner diameter polytetrafluoroethylene inlet at 22 L/min, resulting in a mean (*e*-folding) residence time of 0.22 s. In-flight background determinations were conducted every 60 s by overflowing ultrahigh-purity nitrogen (N_2) at the entrance of the ion molecule reaction (IMR) region, which we demonstrate represents the dominant surface source of residual signals following encounters of polluted air masses. To reduce the difference in water vapor pressure between ambient measurements and background determinations, which affects the instrument sensitivities (Kercher et al., 2009; Lee et al., 2014), the IMR region was continuously humidified with 100 cm^3/min STP of saturated ultrahigh-purity nitrogen N_2 flow resulting in about 0.15 torr of constant water vapor pressure in the IMR region. The IMR region is maintained close to 75 torr with a mean residence time of ~30 ms.

Different techniques were employed to determine HRToF-CIMS sensitivity and its dependence on water vapor pressure, depending on availability of the calibrant gas. Cl_2 and SO_2 were calibrated using calibrated using a permeation device (96 ng/min, KIN-TEK) whose output was veried by gravimetric analysis. HOCl was calibrated following the protocol described by Foster et al. (1999). HCl was calibrated using microinjections of methanol solutions of known HCl concentrations (Sigma-Aldrich), as described by Lee et al. (2014). We relied on the iodide ionization sensitivity to $BrNO_2$ determined by quantum chemical calculations described by Iyer et al. (2016), scaled by the ratio of the calculated to measured sensitivities to $ClNO_2$. For BrCl, we applied the mean of the measured sensitivities of Cl_2 (2.9 counts per second per ppt normalized to a million total reagent ion counts per second, or ncps/ppt) and Br_2 (2.0 ncps/ppt) of 2.5 ncps/ppt, which is comparable to the sensitivity obtained by quantum chemical calculation of 3.0 ncps/ppt (Iyer et al., 2016). The dependence of the sensitivity on water vapor pressure was determined by varying the humidity level of the overflow gas into which the calibrant gases were diluted. We

estimate a 30% uncertainty for those species that were directly calibrated and 50% for $BrNO_2$. These levels of uncertainty do not significantly impact the main findings reported below, which are that (i) Br_2, $BrNO_2$, and BrCl together far exceed—even after accounting for measurement uncertainty—the amount of bromine expected given the observed amounts of chlorine species and typical bromine to chlorie ratios found in U.S. coal and that (ii) such encounters were observed in only the air masses originating from coal-fired power plants without wet flue gas desulfurization (FGD) but not others that employed wet FGD or in exhaust from power plants utilizing fuels other than coal.

The 1-s HRToF-CIMS detection limits (3σ) for HCl, HOCl, Cl_2, $ClNO_2$, Br_2, $BrNO_2$, BrCl, and SO_2 are 160, 12, 1.2, 1.8, 1.5, 3.0, 2.7, and 500 ppt, respectively. HBr and HOBr were not detected in power plant exhaust due to spectral interferences from high levels of sulfur oxides clustered with the iodide reagent ion that occur at the same nominal masses. Laboratory (Enami et al., 2007; Huff & Abbatt, 2000; Mochida et al., 1998, 2000; Santschi & Rossi, 2005) and field (Neuman et al., 2010) studies report on the potential for rapid heterogeneous conversion of Cl_2, HOCl, or HOBr to yield a range of bromine containing gaseous species. Though we cannot definitively rule out the possibility of these reactions occurring on the surface of the HRToF-CIMS inlet, it is unlikely that inlet conversion to yield bromine compounds occurred only while sampling the exhaust from coal-fired power plants that were not employing wet FGD technology, as discussed below. Ambient SO_2 was also measured during WINTER by the UV fluorescence technique (Ryerson et al., 1998), and comparison of SO_2 between the two techniques is presented in the manuscript by Lee et al. (2018). The SO_2 data reported here were obtained by the HRToF-CIMS.

Mass concentrations of total submicron nonrefractory particulate chloride (pCl) and sulfate (pSO_4, including organic sulfates) were observed using a high-resolution time-of-flight aerosol mass spectrometer (DeCarlo et al., 2006; Dunlea et al., 2009). Though the suite of instruments on board the C-130 were not able to resolve chloride in refractory and supermicron particles in power plant exhaust with high enough time resolution, it has been extensively reported that coal chloride is emitted primarily as HCl (Herod et al., 1983; Tillman et al., 2009; Tsubouchi et al., 2018; Vassilev et al., 2000). As such, our approach of estimating an upper limit on gaseous bromine species expected in coal-fired power plant exhaust given the sum of the measured chlorine species and the well-established bromide to chloride ratio in U.S. coal is justified, as discussed below. NO_x and NO_y were measured using cavity ring-down spectroscopy (Wild et al., 2014), while carbon monoxide (CO) was measured using vacuum ultraviolet (VUV) resonance fluorescence (Aero-Laser). NO_y was also quantified by two other techniques: (i) by conversion of ambient nitrogen oxides by heated gold catalyst followed by measurement of the resulting NO as well as the ambient NO (Ridley et al., 2004) and (ii) by heating ambient air to 540 °C and subsequently measuring the resulting NO_2 formed as a result of thermal dissociation of nitrogen oxides, as well as the ambient NO_2 (Day et al., 2002; Wooldridge et al., 2010).

3. Results

3.1. Plume Identification and Power Plant Attribution

We identified 50 encounters in which SO_2 mixing ratios were elevated above HRToF-CIMS detection limit (1-s 3σ of ~500 ppt) over a period of several seconds to few minutes, ensuring robust assessment of emission ratios. Mixing ratios of SO_2, pSO_4, HCl, pCl, $ClNO_2$, and Cl_2 as well as the altitude and wind direction during one of those encounters are shown in Figure 1. We present the emission ratio of a compound of interest in supporting information Figure S1 only if its abundance is at least 3 times the instrument level of detection (LOD), and it exhibits a minimum correlation ($R^2 \geq 0.4$) with the tracer of interest such as SO_2. The R^2 of 0.4 was the cutoff above which the orthogonal least squares fit slope was determined to be statistically robust, defined conservatively as when the ratio of the standard error of the slope to the slope was consistently less than 0.1. The median (25th and 75th percentiles) duration of the 50 encounters was about 1.5 min (0.9 and 3.5 min). Using the criterion described above, pSO_4 was the most frequently detected (43 out of 50) of the gaseous or particulate species that was simultaneously enhanced with SO_2 (Figure S1). Four of the seven plume encounters without pSO_4 were due to a lack of time-of-flight aerosol mass spectrometer data because of routine in-flight sampling strategies such as background determinations. We use the phrase *emission ratio* for all reported halogen species for consistency, though whether they are formed during combustion like HCl or produced following the release of precursors into the atmosphere is still unclear. Moreover, ambient levels immediately outside of exhaust plumes originating from power plants were typically below instrument detection limits for some species (e.g., Br_2, $BrNO_2$, and BrCl), suggesting no other sources in the region. Other species (e.g., pCl, $ClNO_2$, pSO_4, and HCl) were on some encounters detected outside of power plant exhaust plumes, indicating additional regional sources. The reported emission ratios were determined as the enhancement relative to SO_2 without forcing the *y*-intercept to 0, as such, represent only the amount due to power plant emissions.

For each plume encounter, we defined a wind sector in which the SO_2 emission source could have resided. This sector originated from the observation point and was drawn initially two transport hours away, determined assuming constant mean wind speed with ±3 standard deviations of the observed wind direction defining the sector boundaries. If the initial sector did not encompass a single operating power plant as reported in the Continuous Emission Monitoring Systems (first quarter of 2015; https://ampd.epa.gov/ampd/) inventory, the sector size was increased by incrementally increasing the transport time by 10 min and angle defining the sector boundaries by 5° until a power plant was captured within the sector. An example of this approach is shown in Figure 2, the wind sector for the polluted air mass encountered on 9 March at around 16:00 (local time) about 150 km east of Pittsburgh, PA. The high levels of SO_2 and halogen containing compounds, high degree of covariance, the direction of the observed winds (Figure 1), and the absence of any other major emission sources in the immediate vicinity (Figure 2) strongly suggest that the intercepted air mass originated from a common source of both species, likely the Homer City power plant, given its proximity (~2.7 km).

Using this wind sector approach, we attributed 12 of the 50 plume encounters to eight unique emission sources (Table 1). The rest (38 out of the 50) were attributed to two or more possible emission sources; that is, more than one power plant source resided in the defined wind sector region. The names of the possible emission source facilities, distances to each from the point of observation, along with the date, time, latitude, longitude, and research flight number of each of the 50 encounters are provided in Table S1, while the observed emission ratios with respect to SO_2 are shown in Figure S1. Comparison between the inventory and observed emission ratios (e.g., CO_2:NO_y, NO_y:SO_2, and CO_2:SO_2) did not provide a clear determination as to which one of the potential power plants in wind sector was responsible for the polluted air mass. Additionally, given the difficulty in modeling plume transport (e.g., using back trajectories) on such fine spatial scales, particularly at nighttime when most of the plume encounters occurred, and the close proximity of many of these power plants to each other relative to the typical variability in the observed wind directions, we did not attempt to parse the list of potential emission sources any further.

Though characterized by elevated levels of SO_2 and observed downwind of at least one operational power plant, contributions to the identified polluted air mass encounters from sources other than power plants cannot be completely ruled out. For instance, plume encounter 11 (Figure S2) observed on 24 February during research flight 7 and attributed solely to the Chambersburg Units 11 and 12 facility, which is further upwind of the city of Chambersburg, PA, relative to the point of observation, exhibited higher CO:NO_y ratios (~3 ppb: ppb) relative to the other plume encounters that were attributed to single emission sources (Table S1), suggesting a possible small contribution from urban sources which are characterized by higher CO/NO_y ratios (CO/NO_x of typically ~10 ppb/ppb or higher; Hassler et al., 2016) relative to those of power plants. During plume 11 encounter, mixing ratios of SO_2, HCl, CO, and NO_y were all elevated during this descent/ascent maneuver, though the temporal variations in SO_2 and HCl were rather distinct from those of CO and NO_y, indicating that though the CO:NO_y emission ratio for this plume encounter was elevated, the HCl and SO_2 likely originated from a source distinct from the nearby urban center. Such encounters highlight the difficulty in attributing a plume encounter to a specific emission source, particularly an air mass observed in the colder wintertime nighttime atmosphere that contain air mass influenced by a suite of combustion sources under a relatively stagnant, shallow boundary layer. pCl and $ClNO_2$ during plume 11 were more correlated with CO and NO_y than with SO_2 and HCl (Figure S2), suggestive of an urban source of pCl and $ClNO_2$. We show examples below of enhancements in pCl and $ClNO_2$ with minimal influence from urban sources.

3.2. HCl in Power Plant Emissions

Ambient levels of HCl were elevated above HRToF-CIMS LOD (1-s 3σ of ~180 ppt) and robustly correlated ($R^2 \geq 0.4$) with SO_2 in 18 of the 50 identified air mass encounters. We report the emission ratio of a compound relative to SO_2 only if this criteria was met (Figure S1). The median (25th and 75th percentiles) HCl:SO_2 emission ratio was 3.3×10^{-2} (2.5×10^{-2} and 5.3×10^{-2}) ppb:ppb, the highest compared to those of pCl, Cl_2, and $ClNO_2$ (Figure 3). The plume encounters in which each compound was robustly detected (≥3 × LOD and R^2

≥ 0.4 with respect to SO_2) and the median emission ratio with respect to SO_2 for each compound are shown in Figure S1.

Of the 50 polluted air mass encounters, 12 were attributed solely to eight unique emission source facilities (Table 1), using the wind trajectory approach detailed above. Six of those 12 exhibited robust levels of HCl (≥3 × LOD and $R^2 \geq 0.4$). Three of those six were attributed to two power plant facilities (Harllee Branch and Homer City) whose HCl:SO_2 emission ratios are reported in the 2011 NEI inventory, allowing a comparison between observations and inventory (Figure S3). Four of the other six plumes were attributed to power plant facilities whose HCl:SO_2 emission ratios were not reported in the 2011 NEI inventory (W H Zimmer, Montour, Chambersburg, and Mountain). The remaining two plumes exhibited enhancements of SO_2 mixing ratios that were so small, the enhancement in HCl would have been below instrument LOD given the reported HCl:SO_2 emission ratios of the source facilities to which they were attributed (P H Glatfelter and Jack McDonough), as shown in Figure S3.

The polluted air masses intercepted downwind of Homer City (plume number 44: 2.7 km, or ~9.0 min assuming constant mean wind speed of 5.0 m/s) and Harllee Branch (plume number 42: 5.2 km, or 19 min assuming constant mean wind speed of 4.4 m/s) exhibited HCl:SO_2 emission ratios of 2.9×10^{-2} and 3.6×10^{-2} ppb:ppb, respectively, with high degrees of correlation between HCl and SO_2 (Table 1). The WINTER observed emission ratios were lower by 13% and 28%, respectively, relative to those reported in the 2011 NEI inventory, possibly reflecting a decrease in HCl relative to SO_2 emissions from these two sources from the period when the 2011 NEI inventory was compiled to when the WINTER observations were con-ducted, but these differences are within the calibration uncertainty of the HRToF-CIMS measurements. Additionally, emissions from power plants can vary over short time periods depending on operating conditions such as efficiency of emission control technology, fuel composition (i.e., halide content of coal which can depend on the mine where the coal was extracted, bituminous vs. subbituminous, etc.), and combustion temperature (Frey & Rubin, 1991; Rubin et al., 1997). Thus, emission ratios may vary over time. Nonetheless, the variability in HCl mixing ratios observed across the 18 air mass encounters with robust HCl (≥3 × LOD and $R^2 \geq 0.4$) was reasonably explained by the HCl expected from the product of the median of HCl:SO_2 emission ratios of all power plants reported in the 2011 NEI inventory (Figure S4a), regardless of fuel combusted, and the observed SO_2 enhanced (ΔSO_2) in each of those 18 plume encounters (Figure S4b), as given by equation (1):

$$\Delta \mathrm{HCl} = \Delta SO_2 \times \mathrm{NEI}\left(\frac{\mathrm{HCl}}{SO_2}\right), \quad (1)$$

where NEI (HCl/SO_2) is a representative HCl:SO_2 emission ratio. The air mass encounters in which HCl was not robustly detected can readily be explained if the power plant emitted HCl at a ratio to SO_2 lower than the median. Power plants tend to be colocated, and reported HCl:SO_2 emission ratios from facilities within a spa-tial cluster can vary over 3 orders of

magnitude (Figure S4a). Thus, our observations will be sensitive to the sources in a given region with the highest HCl:SO_2 emission ratio and likely represent a cluster average.

HCl:SO_2 emission ratios reported in the inventory are generally derived from the flue gas at the source site (https://www.epa.gov/emc/method-26-hydrogen-chloride-halides-halogens). Airborne observations down-wind of the sources, such as those presented here, can be affected by the chemical processing of HCl following its release to the atmosphere. For instance, two air mass encounters both originating from Harllee Branch were intercepted at approximately 5.2 km (plume number 42; Figure S5) and 37.8 km (plume number 43; Figure S6) downwind during the night on research flight 10. The emission ratios with respect to SO_2 decreased for HCl and increased for pCl, $ClNO_2$, and Cl_2 from plume encounters number 42 to 43 (Figure S7). No significant enhancement in CO mixing ratios was observed in either of the plumes (Figures S5 and S6), indicating neither was strongly influenced by urban combustion sources. These observa-tions, therefore, support the production of $ClNO_2$ and Cl_2 in power plant exhaust, consistent with the findings of Riedel et al. (2013), with HCl and pCl presumably acting as their precursors. That is, HCl partitions to the particle phase and $ClNO_2$ is produced by heterogeneous reaction involving N_2O_5 and pCl (Fibiger et al., 2018; Finlayson-Pitts et al., 1989). The decrease in HCl:SO_2 between the two plume encounters was 8.5×10^{-3} ppb:ppb, while the increase in (pCl + $ClNO_2$ + 2 × Cl_2):SO_2 was only 1.8×10^{-3} ppb:ppb, indicating that 6.7×10^{-3} ppb:ppb of chlorine was lost (Figure S7a) due presumably to the formation of another pool of chlorine reservoir species not quantified by the HRToF-CIMS. HCl loss by deposition in the shallow nocturnal surface layer during the ~9-min transport from the emission source to where the plume was intercepted was likely negligible given that its lifetime with respect to deposition is approximately 1 to 2 days (Graedel & Keene, 1995). HCl and $ClNO_2$ were generally the dominant components of Cl_y, with the balance shifting toward $ClNO_2$ and away from HCl with increasing abundances of N_2O_5 and pCl (Figure S8), also consistent with the formation of $ClNO_2$ in power plant exhaust (Riedel et al., 2013). Correcting the observed HCl:SO_2 emission ratio for the Harllee Branch by accounting for HCl loss determined between plume encounters 42 and 43 adds only about 1.2% to the observed emission ratio that is lower than that reported in the 2011 NEI inventory by 28%.

3.3. Bromine in Power Plant Emissions

We identified seven encounters in which Br_2, BrCl, and/or $BrNO_2$ were robustly detected (≥3 × LOD and $R^2 \geq 0.4$ with respect to SO_2), listed in Table 2. Two of those seven were attributed to a sole source (Homer City, Figures 2 and 4; and Harllee Branch, Figure S5) while the rest were attributed to two or more facilities. All potential sources for these seven air mass encounters utilized coal or waste coal as its primary fuel (https://www.eia.gov/; https://ncrdspublic.er.usgs.gov/coalqual/), except for the Armstrong Power facility (natural gas and diesel), which was one of five potential emitting sources for plume encounter 16 (Table 2). According to the U.S. Energy Information Administration (https://www.eia.gov/coal/data/browser/), none of the potential emitting sources listed in Table 2 reported utilizing refined coal, or coal that had been treated with bromide salts prior to combustion, which can increase the likelihood of higher bromine relative to chlorine emissions, during WINTER observations. Six of the seven plume encounters containing Br_y were attributed to at least

one emission source that was not employing wet flue gas desulfurization (Table 1), which efficiently transfers oxidized $HgBr_2$ from gas to liquid phase (McTigue et al., 2014; U.S. EPA, 2015). The exception was air mass encounter number 5, which originated from either the Kyger or Gavin facilities (Figures S9), both of which reported employing wet FGD. The Kyger facility, however, stopped operations on 7 February, the day after the WINTER measurements, which may have impacted the wet FGD operation (ampd.epa.gov/ampd/).

To assess why Br_y species were observed in some but not all encounters, we estimate an upper limit to the total amount of reactive bromine compounds (TRB), including those not measured by the HRToF-CIMS, that could have been present in the intercepted air mass (Figure S10) using the equation below:

$$\mathrm{TRB} = \Delta \mathrm{Cl}_y \times \mathrm{coal}(Br/Cl), \quad (2)$$

where the ΔCl_y is the observed enhancement of reactive chlorine species in each plume encounter, and coal (Br/Cl) is the bromide to chloride ratio characteristic of U.S. coal (~0.02) (Granite et al., 2015; Kolker et al., 2012). The encounter with the highest expected TRB that did not contain any detectable amounts of Br_y was plume encounter number 15, which was observed during nighttime; therefore, loss by photolysis of Br_y during transport would not explain their absence downwind. The expected TRB given the observed enhancement in Cl_y for encounter number 15 was ~148 ppt (equation (2)), which was greater than the expected TRB of six of the seven encounters in which Br_y was actually observed. Encounter number 15 was attributed to the Conemaugh facility (Figure S11), which was employing wet FGD at the time of WINTER. The use of wet FGD, therefore, is likely efficient at removing Br_y from the flue gas prior to their release to the atmosphere.

The median emission ratio of Br_y:SO_2 (where $Br_y = BrCl + BrNO_2 + 2 \times Br_2$) was 1.5×10^{-4} ppb:ppb (Figure 3), roughly 2 orders of magnitude lower than that of HCl:SO_2 (Figure 3). Though the native bromide to chloride content of coal is approximately 0.02, a dominant fraction of the bromine resulting from combustion should be made up of hydrogen bromide (HBr), as with its chlorine counterpart. However, three of the seven encounters in which Br_y was observed exhibited observed levels that exceeded even the total reactive bromine (equation (2)) assuming all of the coal bromide was converted to Br_y (plume encounters 5, 14, and 44), as shown in Figure S10b. Enhancements of Br_y in plume encounters 5 (Figure S9) and 14 (Figure S11) were especially striking, considering that no significant enhancements in HCl, pCl, Cl_2, or $ClNO_2$ were observed. This suggest either that (i) all of the bromide that was present in the coal was converted to Br_2, $BrNO_2$, and BrCl and that there was faster loss of Cl_y relative to Br_y during transport from source to observation point, which is unlikely, or (ii) the bromide to chloride ratio in the fuel was far greater than 0.02. As noted above, no facility reported adding bromide salts to its fuel. Plume encounters 5 and 44 occurred before sunset, which means that the Br_y ratio to SO_2 was much greater at the source than downwind due to loss of Br_y by photolysis.

A remaining question is whether Br_2, $BrNO_2$, and BrCl detected were directly emitted (i.e., following production in the flue gas by the reaction between mercury and bromine radicals;

Jiao & Dibble, 2017) or produced following the emission of their potential precursors (i.e., HBr and/or pBr, neither of which was measured). The only known mechanism for efficient nighttime activation of halogens involve O_3, NO_3, and N_2O_5 (Simpson et al., 2015). However, the levels of N_2O_5 and O_3 at the center of the plumes were depleted relative to the levels outside of the exhaust, that is, were negatively correlated with SO_2 (Table 2), reflecting the elevated levels of NO which reacts rapidly with O_3 and NO_3, the precursors to N_2O_5. Entrainment of O_3 at the edges could lead to N_2O_5 production and chemistry but not in the plume core. When observed, all Br_y species were strongly correlated with SO_2 throughout the plume. That is, they were not elevated only at the plume edges, as would be expected if chemical production occurred via N_2O_5 or O_3 entrainment. This suggests direct emission of Br_y or production by a reaction not involving known N_2O_5-driven chemistry.

4. Summary and Conclusions

We report on measurements of submicron pCl and pSO_4 and reactive gaseous halogen species including HCl, HOCl, Cl_2, $ClNO_2$, BrCl, Br_2, and $BrNO_2$ observed in polluted air mass encounters during the WINTER campaign. A total of 50 plume encounters were identified, characterized by elevated SO_2 mixing ratios observed near and downwind of power plants, located in the northeast United States and also Georgia. Each of the 50 encounters was attributed to one or more operating power generation facilities using a simple wind trajectory approach. To our knowledge, this study represents the most comprehensive airborne assessment of halogen emissions from coal-fired power plants to date. HCl was typically the predominant chlorinecontaining species in the 18 (out of 50) encounters with robust levels of HCl ($\geq 3 \times$ LOD and $R^2 \geq 0.4$ with respect to SO_2) with a median HCl:SO_2 of 3.3×10^{-2} ppb:ppb. The exhaust plumes from two facilities, Homer City in Homer City, PA, and Harllee Branch in Milledgeville, GA, each with HCl:SO_2 emission ratios reported in the 2011 NEI inventory, exhibited robust HCl:SO_2. The observed HCl:SO_2 emission ratios attributed to Homer City and Harllee Branch were lower by 13% and 28%, respectively, relative to those reported in the 2011 NEI inventory for those two facilities, though this bias is within the calibration uncertainty of our instrument. We show evidence that observed plume encounters during WINTER (characterized downwind) may be lower than those reported in the 2011 NEI inventory (characterized at the source site), in part, due to the conversion of HCl to $ClNO_2$ during transport from emission source to observation point. Reactive bromine species (Br_2, $BrNO_2$, and/or BrCl) were detected in seven (out of 50) encounters, likely associated with sources not employing wet FGD emission controls. Three of those seven exhibited Br_y levels that exceeded those expected assuming all of the native bromide in the coal was released to the atmosphere, though none of their potential sources report using bromide salt additives during the time of WINTER. An accurate inventory of halogen emissions from coal-fired power plants, the second largest global source after sea spray, is crucial to assess the impact on regional oxidation and nitrogen cycling. These observations highlight the next challenge, which is to account for fuel composition and emission control technology on halogen emissions.

Supplementary Material

Refer to Web version on PubMed Central for supplementary material.

Acknowledgments

The authors acknowledge the NSF-NCAR Research Aircraft Facility engineers, scientists, pilots, and staff members. Funding for J. A. T. and L. J. was supported by the NSF AGS 1360745. J. C. S., P. C. J., and J. L. J. were supported by NSF AGS-1360834 and NASA NNX15AT96G. D. L. F. was supported by NSF 1433358. WINTER data are available on the NCAR website (http://data.eol.ucar.edu/master_list/?project=WINTER). The views expressed in this article are those of the authors and do not necessarily represent the views or policies of the U.S. Environmental Protection Agency. Mention of trade names, products, or services does not convey, and should not be interpreted as conveying, official EPA approval, endorsement, or recommendation. U.S. EPA had no role in the collection or analysis of data. The EPA role was limited to providing publicly available information on power plants.

References

Behnke W, George C, Scheer V, & Zetzsch C (1997). Production and decay of $ClNO_2$, from the reaction of gaseous N_2O_5 with NaCl solution: Bulk and aerosol experiments. Journal of Geophysical Research, 102(D3), 3795–3804. 10.1029/96jd03057

Chang SY, & Allen DT (2006). Atmospheric chlorine chemistry in southeast Texas: Impacts on ozone formation and control. Environmental Science & Technology, 40(1), 251–262. 10.1021/es050787z [PubMed: 16433359]

Chang SY, McDonald-Buller E, Kimura Y, Yarwood G, Neece J, Russell M, et al. (2002). Sensitivity of urban ozone formation to chlorine emission estimates. Atmospheric Environment, 36(32), 4991–5003. 10.1016/S1352-2310(02)00573-3

Clegg SL, & Brimblecombe P (1985). Potential degassing of hydrogen-chloride from acidified sodium-chloride droplets. Atmospheric Environment, 19(3), 465–470. 10.1016/0004-6981(85)90167-2

Crisp TA, Lerner BM, Williams EJ, Quinn PK, Bates TS, & Bertram TH (2014). Observations of gas phase hydrochloric acid in the polluted marine boundary layer. Journal of Geophysical Research: Atmospheres, 119, 6897–6915. 10.1002/2013jd020992

Day DA, Wooldridge PJ, Dillon MB, Thornton JA, & Cohen RC (2002). A thermal dissociation laser-induced fluorescence instrument for in situ detection of NO_2, peroxy nitrates, alkyl nitrates, and HNO_3. Journal of Geophysical Research, 107(D6), 4046 10.1029/2001jd000779

DeCarlo PF, Kimmel JR, Trimborn A, Northway MJ, Jayne JT, Aiken AC, et al. (2006). Field-deployable, high-resolution, time-of-flight aerosol mass spectrometer. Analytical Chemistry, 78(24), 8281–8289. 10.1021/ac061249n [PubMed: 17165817]

Dunlea EJ, DeCarlo PF, Aiken AC, Kimmel JR, Peltier RE, Weber RJ, et al. (2009). Evolution of Asian aerosols during transpacific transport in INTEX-B. Atmospheric Chemistry and Physics, 9(19), 7257–7287. 10.5194/acp-9-7257-2009

Enami S, Vecitis CD, Cheng J, Hoffmann MR, & Colussi AJ (2007). Global inorganic source of atmospheric bromine. The Journal of Physical Chemistry. A, 111(36), 8749–8752. 10.1021/jp074903r [PubMed: 17713895]

Fibiger DL, McDuffie EE, Dubé WP, Aikin KC, Lopez-Hilfiker FD, Lee BH, et al. (2018). Wintertime overnight NO_X removal in a southeastern United States coal-fired power plant plume: A model for understanding winter NO_X processing and its implications. Journal of Geophysical Research: Atmospheres, 123, 1412–1425. 10.1002/2017jd027768

Finlayson-Pitts BJ, Ezell MJ, & Pitts JN (1989). Formation of chemically active chlorine compounds by reactions of atmospheric Nacl particles with gaseous N_2O_5 and $ClONO_2$. Nature, 337(6204), 241–244. 10.1038/337241a0

Foster KL, Caldwell TE, Benter T, Langer S, Hemminger JC, & Finlayson-Pitts BJ (1999). Techniques for quantifying gaseous HOCl using atmospheric pressure ionization mass spectrometry. Physical Chemistry Chemical Physics, 1(24), 5615–5621. 10.1039/A907362K

Frey HC, & Rubin ES (1991). Probabilistic evaluation of advanced SO_2/NO_X control technology. Journal of the Air & Waste Management Association, 41(12), 1585–1593. 10.1080/10473289.1991.10466954

Good KD, & VanBriesen JM (2016). Current and potential future bromide loads from coal-fired power plants in the Allegheny River basin and their effects on downstream concentrations. Environmental Science & Technology, 50(17), 9078–9088. 10.1021/acs.est.6b01770 [PubMed: 27538590]

Google, (map retrieved on 3 25, 2018). Homer City generating plant, https://goo.gl/maps/JF4xEcCnVFs.

Graedel TE, & Keene WC (1995). Tropospheric budget of reactive chlorine. Global Biogeochemical Cycles, 9(1), 47–77. 10.1029/94gb03103

Granite EJ, Granite EJ, Pennline HW, & Senior C (2015). Mercury control: For coal-derived gas streams, edited, (p. 1 online resource (478 p)). Weinheim, Germany: Wiley-VCH.

Hassler B, McDonald BC, Frost GJ, Borbon A, Carslaw DC, Civerolo K, et al. (2016). Analysis of long-term observations of NO_x and CO in megacities and application to constraining emissions inventories. Geophysical Research Letters, 43, 9920–9930. 10.1002/2016gl069894

Herod AA, Hodges NJ, Pritchard E, & Smith CA (1983). Mass-spectrometric study of the release of HCl and other volatiles from coals during mild heat-treatment. Fuel, 62(11), 1331–1336. 10.1016/S0016-2361(83)80019-2

Huff AK, & Abbatt JPD (2000). Gas-phase Br_2 production in heterogeneous reactions of Cl_2, HOCl, and BrCl with halide-ice surfaces. The Journal of Physical Chemistry. A, 104(31), 7284–7293. 10.1021/jp001155w

Iyer S, Lopez-Hilfiker F, Lee BH, Thornton JA, & Kurten T (2016). Modeling the detection of organic and inorganic compounds using iodide-based chemical ionization. The Journal of Physical Chemistry. A, 120(4), 576–587. 10.1021/acs.jpca.5b09837 [PubMed: 26736021]

Jiao YG, & Dibble TS (2017). First kinetic study of the atmospherically important reactions $BrHg^{\bullet}$ + NO_2 and $BrHg^{\bullet}$ + HOO. Physical Chemistry Chemical Physics, 19(3), 1826–1838. 10.1039/c6cp06276h [PubMed: 28000816]

Keene WC, Khalil MAK, Erickson DJ III, McCulloch A, Graedel TE, Lobert JM, et al. (1999). Composite global emissions of reactive chlorine from anthropogenic and natural sources: Reactive chlorine emissions inventory. Journal of Geophysical Research, 104(D7), 8429–8440. 10.1029/1998JD100084

Kercher JP, Riedel TP, & Thornton JA (2009). Chlorine activation by N2O5: Simultaneous, in situ detection of ClNO2 and N2O5 by chemical ionization mass spectrometry. Atmospheric Measurement Techniques, 2(1), 193–204. 10.5194/amt-2-193-2009

Kolker A, Quick JC, Senior CL, & Belkin HE (2012). Mercury and halogens in coal—Their role in determining mercury emissions from coal combustion. U.S. Geological Survey Fact Sheet, 2012–3122, 1–6. https://pubs.usgs.gov/fs/2012/3122/

Lee BH, Lopez-Hilfiker FD, Mohr C, Kurten T, Worsnop DR, & Thornton JA (2014). An iodide-adduct high-resolution time-of-flight chemical-ionization mass spectrometer: Application to atmospheric inorganic and organic compounds. Environmental Science & Technology, 48(11), 6309–6317. 10.1021/es500362a [PubMed: 24800638]

Lee BH, Lopez-Hilfiker FD, Veres PR, McDuffie EE, Fibiger DL, Sparks TL, et al. (2018). Flight deployment of a high-resolution time-of-flight chemical ionization mass spectrometer: Observations of reactive halogen and nitrogen oxide species. Journal of Geophysical Research: Atmospheres, 123, 7670–7686. 10.1029/2017JD028082

Neuman JA, Nowak JB, Huey LG, Burkholder JB, Dibb JE, Holloway JS, et al. (2010). Bromine measurements in ozone depleted air over the Arctic Ocean, Atmospheric Chemistry and Physics, 10, 6503–6514. 10.5194/acp-10-6503-2010

McCulloch A, Aucott ML, Benkovitz CM, Graedel TE, Kleiman G, Midgley PM, & et al. (1999). Global emissions of hydrogen chloride and chloromethane from coal combustion, incineration and industrial activities: Reactive chlorine emissions inventory. Journal of Geophysical Research, 104(D7), 8391–8403. 10.1029/1999JD900025

McTigue NE, Cornwell DA, Graf K, & Brown R (2014). Occurrence and consequences of increased bromide in drinking water sources. Journal-American Water Works Association, 106(11), E492–E508. 10.5942/jawwa.2014.106.0141

Mielke LH, Furgeson A, & Osthoff HD (2011). Observation of $ClNO_2$ in a mid-continental urban environment. Environmental Science & Technology, 45(20), 8889–8896. 10.1021/es201955u [PubMed: 21877701]

Mochida M, Hirokawa J, & Akimoto H (2000). Unexpected large uptake of O_3 on sea salts and the observed Br_2 formation. Geophysical Research Letters, 27(17), 2629–2632. 10.1029/1999GL010927

Mochida M, Hirokawa J, Kajii Y, & Akimoto H (1998). Heterogeneous reactions of Cl_2 with sea salts at ambient temperature: Implications for halogen exchange in the atmosphere. Geophysical Research Letters, 25(21), 3927–3930. 10.1029/1998GL900100

Osthoff HD, Roberts JM, Ravishankara AR, Williams EJ, Lerner BM, Sommariva R, et al. (2008). High levels of nitryl chloride in the polluted subtropical marine boundary layer. Nature Geoscience, 1(5), 324–328. 10.1038/ngeo177

Read KA, Mahajan AS, Carpenter LJ, Evans MJ, Faria BVE, Heard DE, et al. (2008). Extensive halogen-mediated ozone destruction over the tropical Atlantic Ocean. Nature, 453(7199), 1232–1235. 10.1038/nature07035 [PubMed: 18580948]

Reisch MS (2015). Bromine bails out big power plants. Chemical and Engineering News, 93(11), 17–19.

Ridley B, et al. (2004). Florida thunderstorms: A faucet of reactive nitrogen to the upper troposphere. Journal of Geophysical Research, 109, D17305 10.1029/2004jd004769

Riedel TP, Bertram TH, Crisp TA, Williams EJ, Lerner BM, Vlasenko A, et al. (2012). Nitryl chloride and molecular chlorine in the coastal marine boundary layer. Environmental Science & Technology, 46(19), 10,463–10,470. 10.1021/es204632r [PubMed: 21786750]

Riedel TP, Wagner NL, Dubé WP, Middlebrook AM, Young CJ, Öztürk F, et al. (2013). Chlorine activation within urban or power plant plumes: Vertically resolved $ClNO_2$ and Cl_2 measurements from a tall tower in a polluted continental setting. Journal of Geophysical Research: Atmospheres, 118, 8702–8715. 10.1002/jgrd.50637

Robbins RC, Cadle RD, & Eckhardt DL (1959). The conversion of sodium chloride to hydrogen chloride in the atmosphere. Journal of Meteorology, 16(1), 53–56. 10.1175/1520-0469(1959)016<0053:TCOSCT>2.0.CO;2

Roberts JM, Osthoff HD, Brown SS, & Ravishankara AR (2008). N_2O_5 oxidizes chloride to Cl_2 in acidic atmospheric aerosol. Science, 321(5892), 1059–1059. 10.1126/science.1158777 [PubMed: 18599742]

Rossi MJ (2003). Heterogeneous reactions on salts. Chemical Reviews, 103(12), 4823–4882. 10.1021/cr020507n [PubMed: 14664635]

Rubin ES, Kalagnanam JR, Frey HC, & Berkenpas MB (1997). Integrated environmental control modeling of coal-fired power systems. Journal of the Air & Waste Management Association, 47(11), 1180–1188. 10.1080/10473289.1997.10464063

Ryerson TB, Buhr MP, Frost GJ, Goldan PD, Holloway JS, Hübler G, et al. (1998). Emissions lifetimes and ozone formation in power plant plumes. Journal of Geophysical Research, 103(D17), 22,569–22,583. 10.1029/98jd01620

Saiz-Lopez A, & von Glasow R (2012). Reactive halogen chemistry in the troposphere. Chemical Society Reviews, 41(19), 6448–6472. 10.1039/c2cs35208g [PubMed: 22940700]

Santschi C, & Rossi MJ (2005). The heterogeneous interaction of HOCl with solid KBr substrates: The catalytic role of adsorbed halogens. Physical Chemistry Chemical Physics, 7(13), 2599–2609. 10.1039/b503071d [PubMed: 16189570]

Schroeder WH, Anlauf KG, Barrie LA, Lu JY, Steffen A, Schneeberger DR, & et al. (1998). Arctic springtime depletion of mercury. Nature, 394(6691), 331–332. 10.1038/28530

Simpson WR, Brown SS, Saiz-Lopez A, Thornton JA, & von Glasow R (2015). Tropospheric halogen chemistry: Sources, cycling, and impacts. Chemical Reviews, 115(10), 4035–4062. 10.1021/cr5006638 [PubMed: 25763598]

Tanaka PL, Riemer DD, Chang S, Yarwood G, McDonald-Buller EC, Apel EC, et al. (2003). Direct evidence for chlorine-enhanced urban ozone formation in Houston, Texas. Atmospheric Environment, 37(9–10), 1393–1400. 10.1016/S1352-2310(02)01007-5

Thornton JA, Kercher JP, Riedel TP, Wagner NL, Cozic J, Holloway JS, et al. (2010). A large atomic chlorine source inferred from mid-continental reactive nitrogen chemistry. Nature, 464(7286), 271–274. 10.1038/nature08905 [PubMed: 20220847]

Tillman DA, Duong D, & Miller B (2009). Chlorine in solid fuels fired in pulverized fuel boilers—Sources, forms, reactions, and consequences: A literature review. Energy & Fuels, 23(7), 3379–3391. 10.1021/ef801024s

Tsubouchi N, Mochizuki Y, Wang YH, & Ohtsuka Y (2018). Fate of the chlorine in coal in the heating process. ISIJ International, 58(2), 227–235. 10.2355/isijinternational.ISIJINT-2017-302

United States Environmental Protection Agency (2015). Sources contributing inorganic species to drinking water intakes during low flow conditions on the Allegheny River in western Pennsylvania, edited by O. o. R. a. Development. United States Office of Energy Markets and End Use. Annual energy review, edited, p. volumes, Energy Information Administration, Office of Energy Markets and End Use, Washington, D.C.

Vassilev SV, Eskenazy GM, & Vassileva CG (2000). Contents, modes of occurrence and behaviour of chlorine and bromine in combustion wastes from coal-fired power stations. Fuel, 79(8), 923–937. 10.1016/S0016-2361(99)00231-8

Vogt R, Crutzen PJ, & Sander R (1996). A mechanism for halogen release from sea-salt aerosol in the remote marine boundary layer. Nature, 383(6598), 327–330. 10.1038/383327a0

Warneke C, Trainer M, de Gouw JA, Parrish DD, Fahey DW, Ravishankara AR, et al. (2016). Instrumentation and measurement strategy for the NOAA SENEX aircraft campaign as part of the Southeast Atmosphere Study 2013. Atmospheric Measurement Techniques, 9(7), 3063–3093. 10.5194/amt-9-3063-2016 [PubMed: 29619117]

Wild RJ, Edwards PM, Dubé WP, Baumann K, Edgerton ES, Quinn PK, et al. (2014). A measurement of total reactive nitrogen, NO_y, together with NO_2, NO, and O_3 via cavity ring-down spectroscopy. Environmental Science & Technology, 48(16), 9609–9615. 10.1021/es501896w [PubMed: 25019919]

Wooldridge PJ, Perring AE, Bertram TH, Flocke FM, Roberts JM, Singh HB, et al. (2010). Total peroxy nitrates (sigma PNs) in the atmosphere: The thermal dissociation-laser induced fluorescence (TD-LIF) technique and comparisons to speciated PAN measurements. Atmospheric Measurement Techniques, 3(3), 593–607. 10.5194/amt-3-593-2010

Young CJ, Washenfelder RA, Roberts JM, Mielke LH, Osthoff HD, Tsai C, et al. (2012). Vertically resolved measurements of nighttime radical reservoirs in Los Angeles and their contribution to the urban radical budget. Environmental Science & Technology, 46(20), 10,965–10,973. 10.1021/es302206a [PubMed: 21786750]

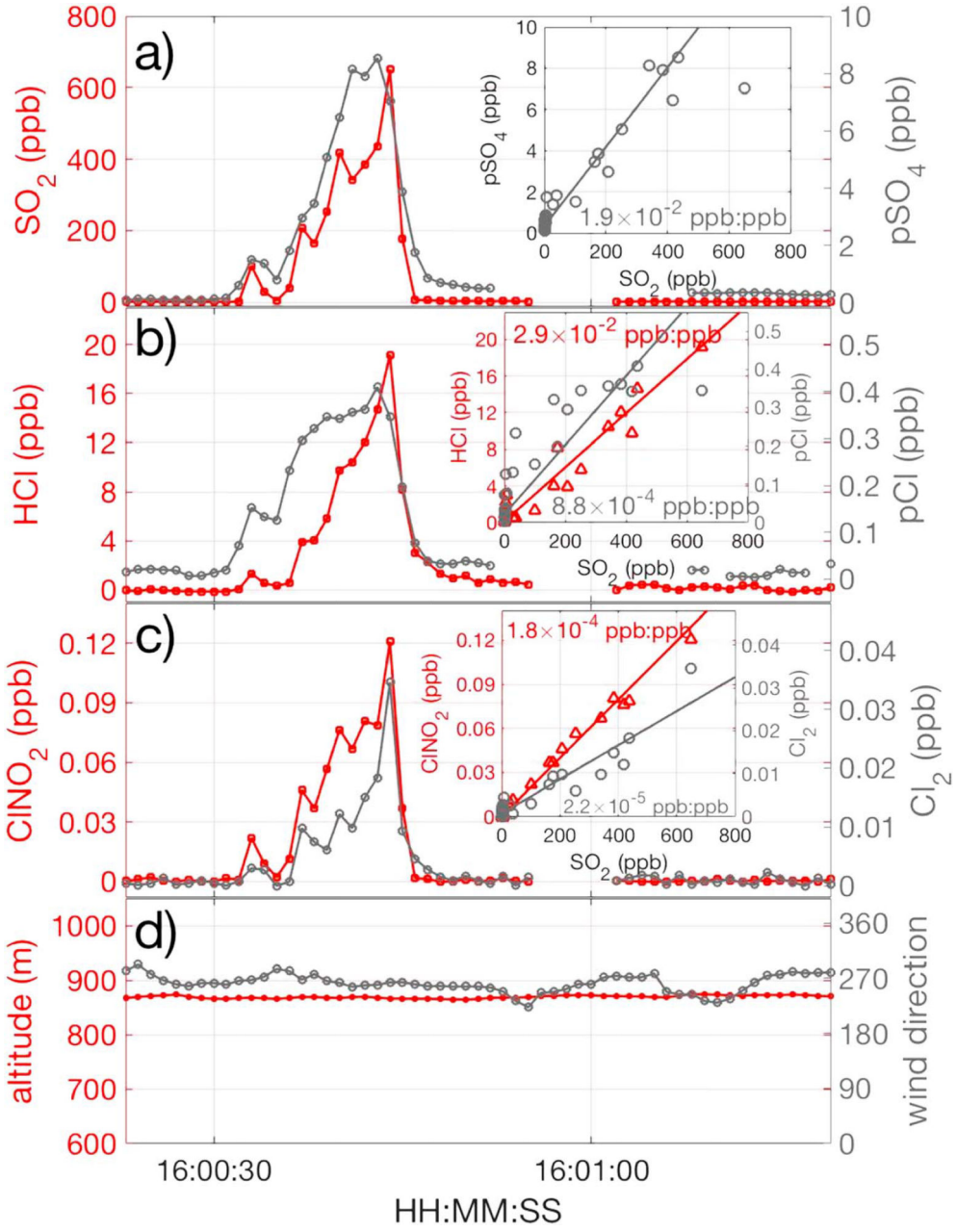

Figure 1.

Mixing ratios of (a) SO_2, pSO_4; (b) HCl, pCl; (c) $ClNO_2$, and Cl_2 during research flight 11 on 9 March around 4 p.m. local time (polluted plume encounter number 44 out of 50; see Table S1). The slopes with respect to SO_2 shown in the insets of (a), (b), and (c) define the corresponding emission ratios with respect to SO_2. Altitude and wind direction during this polluted air mass encounter are shown in (d).

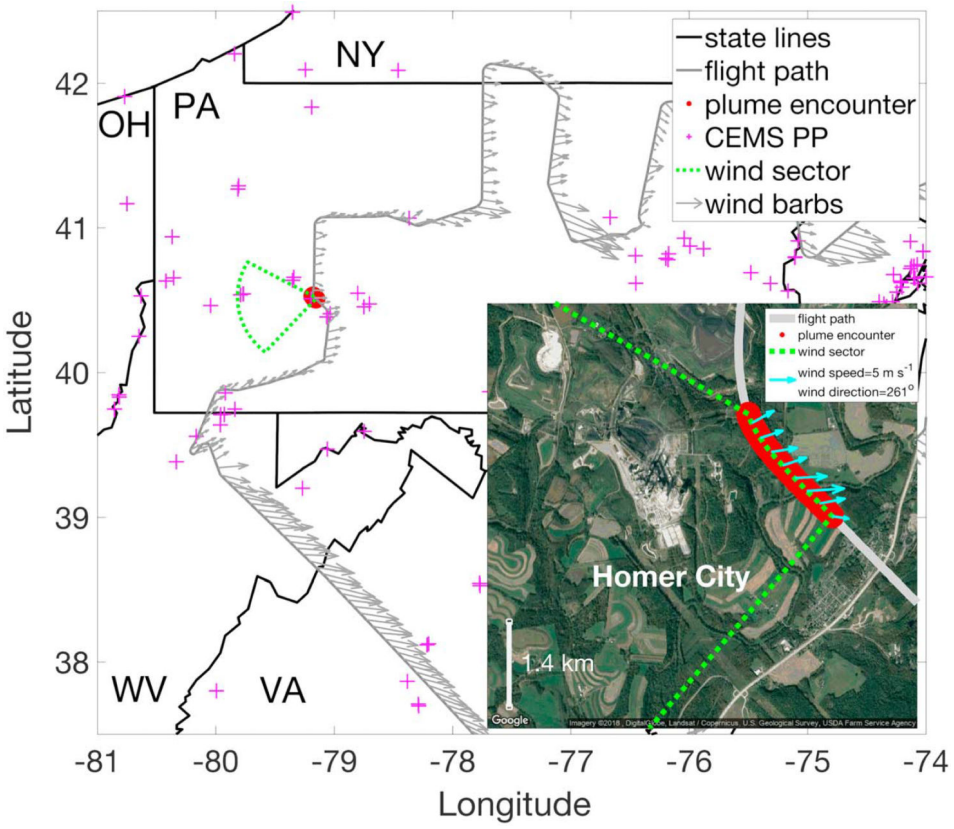

Figure 2.

Flight path of the C-130 aircraft (gray) during research flight 11 on 9 March (polluted plume encounter number 44). The inset shows a close-up of the flight path when the polluted air mass encounter shown in Figure 1 occurred (red in both the main figure and inset), with the wind sector (green) in which the potential emission sources reside. This plume encounter (plume number 44; see Table S1) was attributed to the Homer City power plant given that the facility was just ~2.7 km away (~0.15 hr plume travel time assuming the observed wind speed and direction stayed constant) from where the air mass was observed and the high levels of SO_2 and halogen-containing compounds (Figure 1), and given that the next closest power plants in the wind sector was ~50 km away. Inset image was obtained on 25 March 2018 (Google, 2018). CEMS PP = Continuous Emission Monitoring Systems power plant; OH = Ohio; PA = Pennsylvania; NY = New York; WV = West Virginia; VA = Virginia.

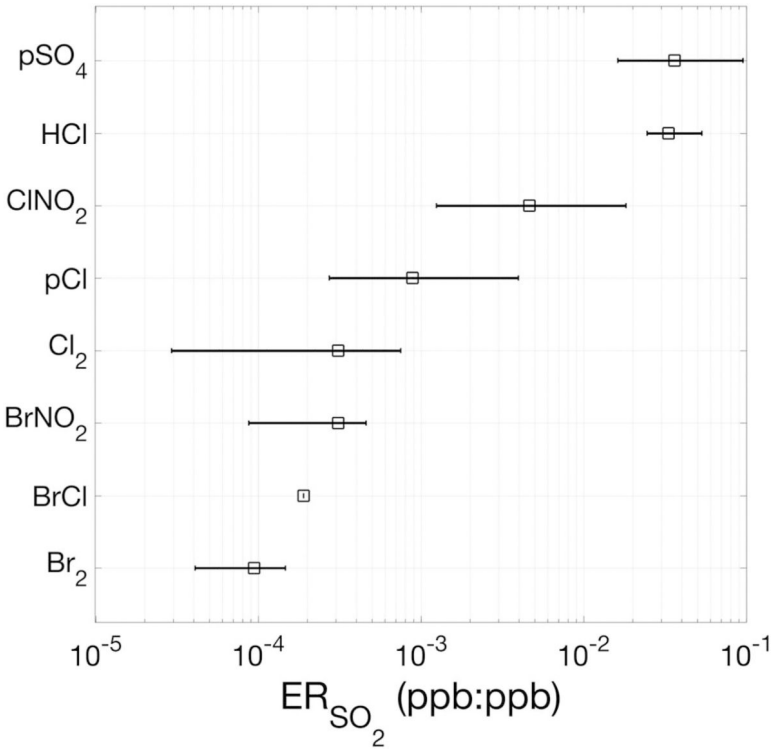

Figure 3.

Median emission ratios of pSO_4, HCl, $ClNO_2$, pCl, Cl_2, $BrNO_2$, BrCl, and Br_2 for the plume encounters in which each was robustly detected (≥ 3 × LOD and R^2 ≥ 0.4 with respect to SO_2). The horizontal bars represent the 25th and 75th percentiles of the qualifying emission ratios. The number of plume encounters in which each compound was robustly detected is shown in Figure S1. LOD = level of detection.

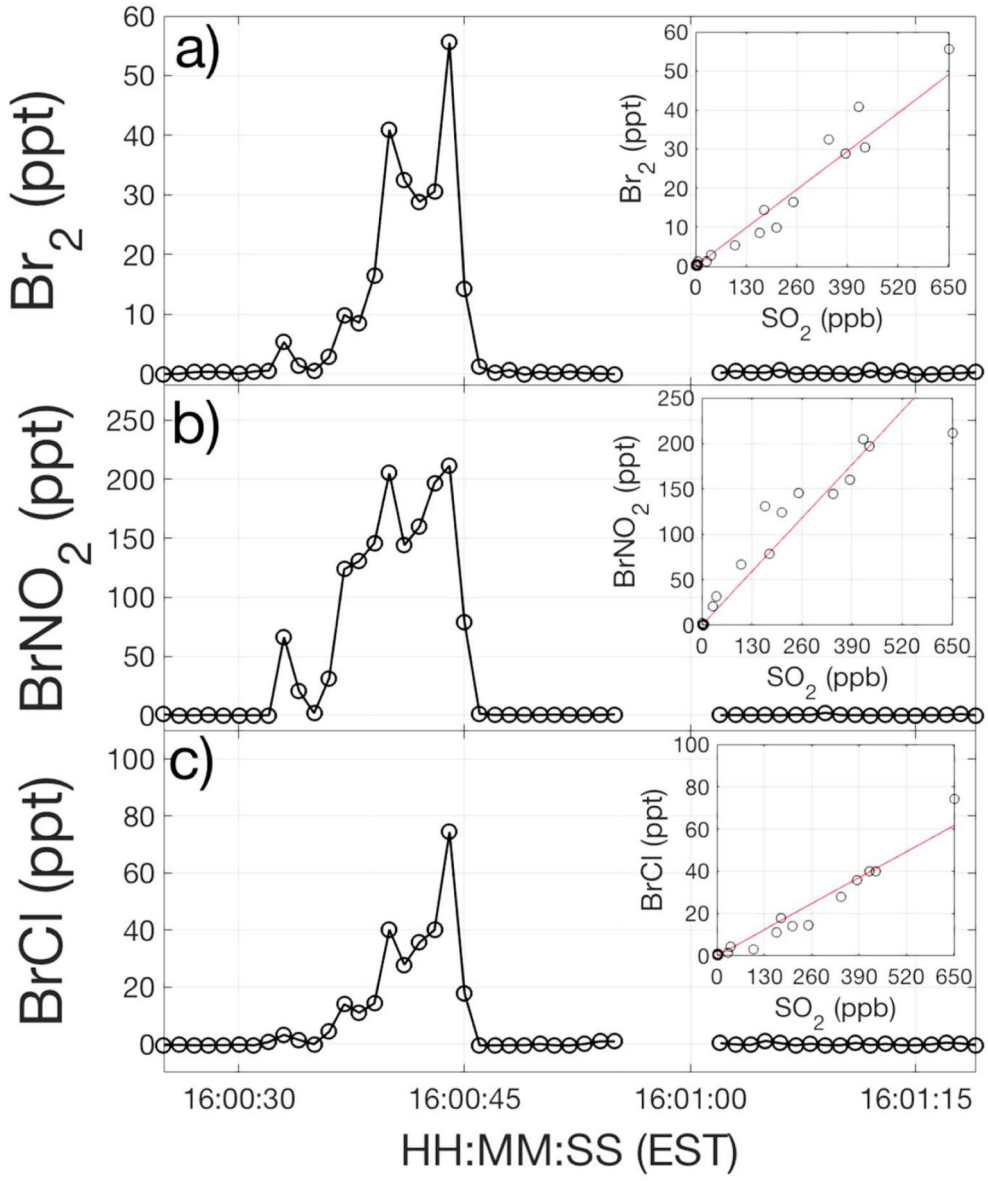

Figure 4.

Mixing ratios of (a) Br_2, (b) $BrNO_2$, and (c) BrCl observed during the same plume encounter as shown in Figure 1. The insets show the corresponding comparison to SO_2.

Table 1

The Names of the Power Plants, the Fuel(s) Utilized by the Facility, Observed HCl:SO_2 Emission Ratios, the Standard Error Associated With the Emission Ratios, and the Correlation Coefficient Between HCl and SO_2 (R^2) for the Plume Encounters That Were Attributed to a Single Power Plant

Plume number	Name of emission source (state)	Fuel utilized	Observed HCl:SO_2 emission ratio ± standard error (R^2) (ppt:ppb)
2	W H Zimmer (OH)	Coal/natural gas	14.5 ± 2.6 (0.15)
4	P H Glatfelter (OH)	Coal/diesel	7.3 ± 4.6 (0.03)
11	Chambersburg 12 and 13 (PA)	Natural gas	53.0 ±1.4 (0.81)
12	Chambersburg 12 and 13 (PA)	Natural gas	53.1 ± 2.0 (0.73)
13	Mountain (PA)	Natural gas/distillate fuel oil	74.8 ± 1.2 (0.96)
39	Jack McDonough (GA)	Diesel/natural gas	23.5 ± 13.2 (0.04)
40	Jack McDonough (GA)	Diesel/natural gas	8.4 ± 22.4 (0.00)
41	Jack McDonough (GA)	Diesel/natural gas	17.6 ± 15.6 (0.02)
42	Harllee Branch (GA)	Coal	35.6 ± 1.4 (0.95)
43	Harllee Branch (GA)	Coal	27.1 ± 2.7 (0.69)
44	Homer City (PA)	Coal	28.8 ± 1.3 (0.94)
45	Mountour (PA)	Coal	0.7 ± 1.1 (0.00)

Note. OH = Ohio; PA = Pennsylvania; GA = Georgia.

Table 2

Plume Encounters That Exhibited Elevated Levels of at Least One of the Three Reactive Bromine Compounds (Br_2, $BrNO_2$, and BrCl) Detected by the HRToF-CIMS

Plume #	RF # date time (EST)	N_2O_5:SO_2 (ppb:ppb) mean N_2O_5 at edge (ppt) $R(N_2O_5$ vs. $SO_2)$	Br_y:SO_2 (ppb:ppb)	Distance (km) and time (hr) since emission	Plant(s)	Coal type	SO_2 control technology
5	RF 2	-1.0×10^{4} ppb:ppb 10 ppt	2.1×10^{-4}	3.8 km 0.3 hr	Gavin	Bituminous, subbituminous	Wet FGD
	6 February 17:02	−0.83		6.0 km 0.4 hr	Kyger	Bituminous, subbituminous	Wet FGD
9	RF 2	8.0×10^{-4} ppb:ppb 29 ppt	6.1×10^{-4}	11.9 km 0.4 hr	Grant	Bituminous waste coal	No FGD Reagent injection
	6 February 18:25	0.73		35.6 km 1.3 hr	Harrison	Bituminous	Wet scrubbers
14	RF 7	-1.1×10^{-2} ppb:ppb 670 ppt	1.5×10^{-4}	11.3 km 0.7 hr	Roxboro	Bituminous, subbituminous	Wet FGD
	24 February 6:52	−0.85		22.5 km 1.3 hr	CPI USA Roxboro	Bituminous, biomass	No FGD
				27.1 km 1.6 hr	Mayo	Bituminous, subbituminous	Wet FGD
16	RF 9	-4.0×10^{-4} ppb:ppb 28 ppt	0.25×10^{-4}	18.0 km 0.9 hr	Seward	Bituminous waste coal	Dry scrubber (#1 and 2)
	3 March 2:42	−0.34		19.1 km 1.0 hr	Conemaugh	Bituminous	Wet FGD
				35.8 km 1.8 hr	Homer City	Bituminous	Dry FGD (Units 1 and 2) Semidry FGD (Unit 3)
				54.7 km 2.8 hr	Armstrong Power, LLC	Natural gas/diesel	No FGD Reagent injection
				55.7 km 2.8 hr	Keystone	Bituminous	Wet FGD
21	RF 9	2.0×10^{-4} ppb:ppb 86 ppt	0.40×10^{-4}	54.2 km 8.2 hr	Ebensburg	Waste coal (bituminous)	No FGD Reagent injection
	3 March 4:29	0.10		54.4 km 8.3 hr	Cambria	Waste coal (bituminous)	No FGD Reagent injection
42	RF	-7.1×10^{-3} ppb:ppb 618 ppt	0.38×10^{-4}	5.2 km 0.32 hr	Harllee Branch	Bituminous	No FGD
	March 3:35	−0.51					
44	RF 11	0 ppb:ppb 2 ppt	7.0×10^{-4}	2.7 km 0.15 hr	Homer City Generating Station	Bituminous	Dry FGD (Units 1 and 2) Semi-dry FGD (Unit 3)
	9 March 16:00	−0.18					

Note. We define Br_y as the sum of these three species. The times since emission were calculated assuming that the observed wind speed at the plume intercept location remained constant. HRToF-CIMS = high-resolution time of flight chemical ionization spectrometer; FGD = flue gas desulfurization; EST = Eastern Standard Time.